

High- Q cavity-induced synchronization in oscillator arrays

Giovanni Filatrella^{1,*} Niels Falsig Pedersen,^{2,†} and Kurt Wiesenfeld^{3,‡}

¹Unità INFN Salerno and Facoltà di Scienze, Università del Sannio, Via Caio Ponzio Telesino 11, I-82100 Benevento, Italy

²Department of Electric Power Engineering, The Technical University of Denmark, DK-2800 Lyngby, Denmark

³School of Physics, Georgia Institute of Technology, Atlanta, Georgia 30332

(Received 24 June 1999; revised manuscript received 4 October 1999)

A model for a large number of Josephson junctions coupled to a cavity is presented. The system displays synchronization behavior very similar to that reported in recent experiments [P. Barbara *et al.*, Phys. Rev. Lett. **82**, 1963 (1999)]. The essential dynamical mechanism responsible for coherence should be generic in nonlinear oscillator systems where the interactions are mediated by a highly resonant cavity, in analogy with gas lasers.

PACS number(s): 05.45.Xt, 74.50.+r

I. INTRODUCTION

One of the most widely cited types of self-organized dynamical behavior is that of spontaneous synchronization in a population of nonlinear oscillators. Well known examples include the flashing of fireflies, networks of neurons and cardiac pacemaker cells, chorusing crickets, laser arrays, and Josephson junction arrays [1–5]. Features common to these and other such systems can be understood in fairly general terms, most famously embodied by a model introduced by Kuramoto [6]. The Kuramoto model explains how mutually interacting oscillators, each of which has a different natural frequency, can undergo a sharp macroscopic transition from a disordered to a coherent dynamical state when the coupling constant exceeds a critical threshold.

Recently [7], laboratory experiments on two-dimensional Josephson arrays revealed a synchronization transition with unique properties. These experiments approached the synchronization problem in an interesting way, namely by increasing the number N of active oscillators (rather than tuning a global parameter). As N passed a critical value, the amount of detected power increased dramatically; moreover, the conversion efficiency from dc to ac power was unusually large compared to most other Josephson array experiments. An important distinguishing feature of the experimental design was the existence of a strongly resonant cavity. Barbara *et al.* suggest that this provides the essential mechanism operating in their experiments. A somewhat related experiment was performed with a long Josephson junction interacting with a high- Q cavity [8,9], and also in this case the results clearly showed an enhancement in the phase-locking due to the cavity. In these latter experiments, however, the threshold for the onset of the fully phase-locked state as in [7] was not observed.

Arrays of Josephson junctions coupled to a cavity thus seem to have striking similarities with the laser: they consist of oscillators that would radiate incoherently if not for the presence of a tuned cavity. Barbara *et al.* employed this anal-

ogy to underline the remarkable similarities between the two systems; they pointed out that this analogy has been noted by others [10,11], and as early as Tilley [12].

The purpose of the present paper is to investigate the role of resonant cavity enhancement of synchronization from the perspective of nonlinear dynamics. The resonant cavity adds a crucial new element to the frequency-locking mechanism which is missing from traditional treatments. We explore this mechanism both by studying a specific circuit model for the Josephson array, and by developing the connection with a modified version of the Kuramoto model. Thus, the main features are expected to be applicable in general to oscillator arrays coupled via a strong resonance. The advantage of the specific example of the Josephson array is that it lets us explore the phenomenon in some depth.

II. MODEL AND SIMULATIONS

Our circuit model is depicted in the inset of Fig. 1. We consider an array of N Josephson junctions coupled via capacitors to a resonant RLC load. The underdamped junctions are current biased in the hysteretic part of the I - V curve, so that a given junction can be put in either the zero or finite-

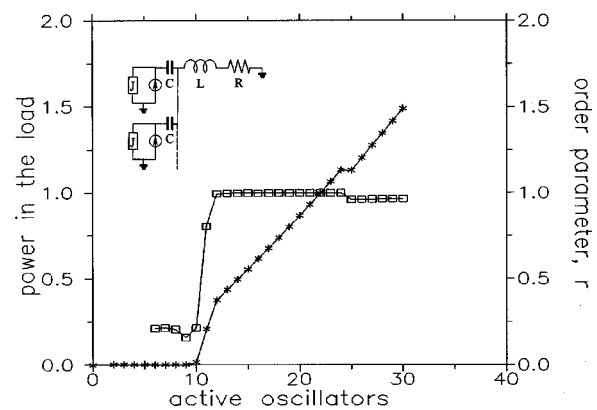


FIG. 1. Load power (stars, left axis) in normalized units and Kuramoto order parameter (squares, right axis) versus number of active junctions for a parallel array. The inset shows the circuit schematic. Parameters of the simulations are $N=30$, $\beta=10$, $\gamma=0.003$, $\delta=0.006$, $\beta_L=1$, $Q=100$.

*Electronic address: giofil@physics.unisa.it

†Electronic address: nfp@eltek.dtu.dk

‡Electronic address: kurt.wiesenfeld@physics.gatech.edu

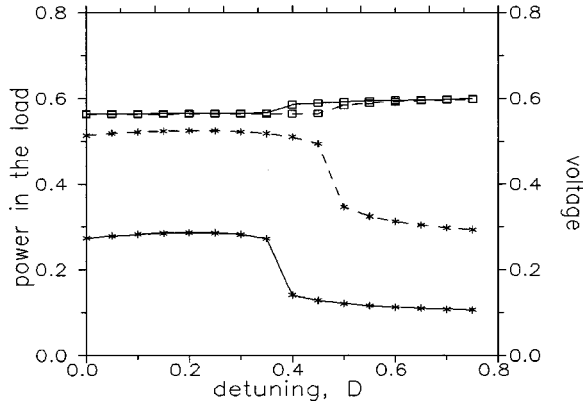


FIG. 2. Load power (stars, left axis) and voltage (squares, right axis) versus detuning D . The solid line refers to the case with two active oscillators, and the dashed lines to three active oscillators. All quantities are plotted in normalized units. Parameters of the simulations are $N=3$, $\beta=10$, $\delta=0.1$, $\beta_L=1$, $Q=100$.

voltage state—only the latter corresponds to an active oscillator, which allows us (as in the experiments [7]) to change the number of active oscillators N_a by selecting the appropriate initial conditions. In our simulations the critical currents are chosen at random from a distribution with a fixed width (as would be the case for any fabricated array with many junctions). The distribution of critical currents leads to a distribution of natural frequencies; consequently, only through their nonlinear interactions can any frequency locking occur.

Figure 1 plots the power dissipated in the RLC load as a function of N_a as determined from numerical simulations. There is a clear threshold above which the load becomes active. To gain some insight into what the individual junctions are doing, we also plot an order parameter $r = (1/N_a) \sum_j \exp(i\phi_j)$ where ϕ_j is the phase of the macroscopic wave function across the j th junction. This quantity (by definition $0 \leq r \leq 1$) jumps from a very low value to essentially unity. Thus, the threshold observed in the load power coincides with the sudden onset of complete coherence (frequency and phase locking). Moreover, the maximum conversion efficiency from dc to ac power is quite large at 14% for the example in Fig. 1, as compared with 17% and 5% reported in Ref. [7]. A similar model of soliton oscillators coupled in parallel to a cavity was introduced in [8,9]. It was shown that the interaction through the cavity was strong enough to force phase locking also for junctions with different natural oscillation frequencies [13].

The simulations shown in Fig. 1 also provide a key insight as to the essential dynamics of the transition. Above threshold, as we successively add one more active oscillator to the system, the power in the load jumps by a fixed amount. Since it is the load that mediates the coupling between elements, this means that the coupling strength itself increases with each additional synchronized oscillator. To better visualize the effect, we have run a simulation with just two and three identical junctions. We have then smoothly changed the critical current of one oscillator, and observed the behavior of the power dissipated in the load and of the average voltage. The result is shown in Fig. 2, where we have plotted the average voltage across an oscillator (squares) as a function of the detuning D . The detuning is

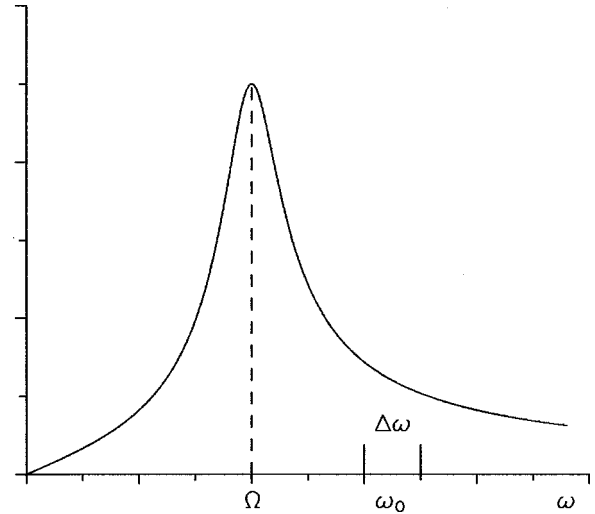


FIG. 3. Schematic (in arbitrary units) illustrating the essential elements of a cavity-induced synchronization mechanism: a sharp cavity resonance (peaked at Ω) and an off-resonance distribution of oscillator frequencies (center ω_0 , width $\Delta\omega$).

defined in such a way that for $D=0$ the first oscillator has the same natural frequency of the others, and for $D=1$ it has the maximum difference. It is clear that the system with three oscillators is able to keep the oscillators locked for a wider range of detuning. It is also clear why this is so: the cavity loaded with a larger number of oscillators can deliver more power (measured as the power dissipated in the load, i.e., the stars in Fig. 2) and therefore is able to overcome a larger amount of disorder in the critical currents.

The simulations lead us to the qualitative picture depicted in Fig. 3. Sketched is a resonance curve representing the cavity response (peak at Ω), together with an interval (width $\Delta\omega$) indicating the range of natural (i.e., uncoupled) frequencies of the active oscillators. As each off-resonance oscillator is added, the power in the load builds gradually, and as the load oscillations grow, they pull the individual oscillator frequencies toward the cavity resonance Ω . This continues until the cavity oscillation is large enough that one oscillator locks to the frequency Ω . This event substantially increases the amplitude of the load oscillations, so that additional oscillators are pulled into the locked state. This mechanism provides a strong feedback mechanism which is absent in a low- Q cavity.

This idea can be made quantitative by analyzing the equations governing the dynamics of the circuit in Fig. 1. In dimensionless form, they are

$$\beta \ddot{\phi}_j + \dot{\phi}_j + I_j \sin \phi_j = I - \dot{q}_j, \quad (1)$$

$$\ddot{P} + \frac{R}{L\omega_{rc}} \dot{P} + \frac{1}{LC\omega_{rc}^2} q_j = \frac{1}{\beta_L} \dot{\phi}_j, \quad (2)$$

where $j=1, \dots, N$, and β is the junction capacitance, I_j is the critical current, I is the bias current, q_j is the charge on the j th coupling capacitor, P is the total charge on the load capacitors, c is the coupling capacitance, and L , R , and C are the load inductance, resistance, and capacitance, respectively. To make the equations dimensionless we have used

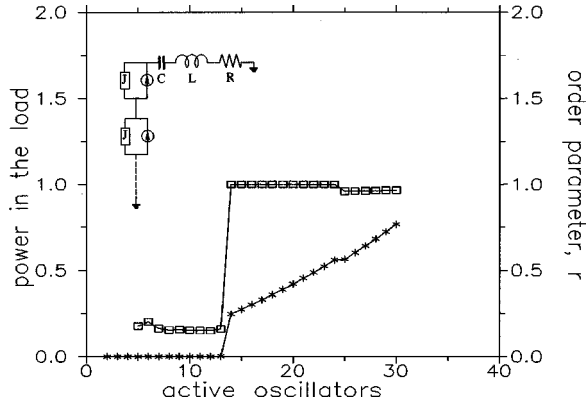


FIG. 4. Load power (stars, left axis) in normalized units and Kuramoto order parameter (squares, right axis) versus the number of active junctions for a series array. The inset shows the circuit schematic. Parameters of the simulations are $N=30$, $\beta=10$, $\gamma=0.003$, $\delta=0.1$, $\beta_L=0.1$, $Q=100$.

the frequency $\omega_{rc}=2eRI_0/\hbar$ and the analogous of the superconducting quantum interference device (SQUID) parameter $\beta_L=\hbar/2eLI_0$. The distribution $\mathcal{P}(I_j)$ of the critical currents is assumed Lorentzian around an average value \bar{I} : $\mathcal{P}(I_j)=(\gamma/\pi)[\gamma^2+(I-I_j)^2]^{-1}$. We note, first, the familiar fact that the junctions do not directly couple to each other [8], but rather couple to the load which then acts back on the junctions, in this case through the coupling capacitors. The key point is this: when the load has a sharp resonance, it acts not merely as a coupling medium, but it's role as an active dynamical entity becomes crucial. Summing the second equation over all j yields

$$\ddot{P} + 2\Gamma\dot{P} + \Omega^2 P = 1/(N\beta_L) \sum_{k=1}^N \dot{\phi}_k, \quad (3)$$

where we have introduced the damping parameter $\Gamma=R/2L$ and the resonant frequency $\Omega=\sqrt{1/LC}$. The junction oscillations serve to drive the load oscillations, which feed back on the junction dynamics, and in the absence of a strong cavity resonance each (active) junction affects the load (and thus each of the other junctions) with roughly the same strength. In contrast, for a high- Q load those junctions locked at the resonance frequency drive the load much harder than junctions which are not locked (and so off-resonance). Consequently, the locked junctions interact far more strongly with the array.

To make sure that the mechanism we are presenting here is general enough, we have also run simulations with *series* arrays, i.e., with the more traditional scheme [14]:

$$\beta\ddot{\phi}_j + \dot{\phi}_j + I_j \sin \phi_j = I - \dot{q}_j \quad (4)$$

$$\ddot{q} + \frac{R}{L\omega_{rc}}\dot{q} + \frac{1}{LC\omega_{rc}^2}q = \frac{1}{\beta_L} \sum_{i=1}^N \dot{\phi}_i. \quad (5)$$

The simulation results are shown in Fig. 4, together with a sketch of the series circuit. We notice that although the quantitative picture may be different, the qualitative features are the same as Fig. 1, thus suggesting that the same general mechanism is at work.

III. A GENERAL FRAMEWORK

In view of the generality of the observed phenomenon, we would like to draw a connection with a generic model describing synchronization. Undoubtedly, the best known such model was introduced by Kuramoto [6,15]

$$\dot{\theta}_j = \omega_j - (K/N) \sum_{i=1}^N \sin(\theta_j - \theta_i + \alpha). \quad (6)$$

In fact, a rigorous condition between the overdamped series arrays [Eqs. (4) and (5) with $\beta=0$] and the Kuramoto model, Eq. (6), has been demonstrated previously [16]. We have not been able to provide a similarly careful reduction of the more general Josephson systems (1) and (2) and (4) and (5). In what follows, we have a more humble goal. Namely, we want to capture the essential features of the new synchronization mechanism by an appropriate modification of the generic model. Our remarks parallel the analysis of Ref. [16]; the basic picture, we believe, remains unaltered for underdamped junctions in the parallel biasing scheme of Fig. 1.

In general the variables θ_j in Eq. (6) represent a reparametrization of the limit cycle in the uncoupled limit, such that the uncoupled oscillator undergoes uniform angular velocity around the limit cycle. Although this variable is well defined mathematically, in general it is not easy to write down the explicit transformation from the original dynamical variables [the ϕ_j of Eq. (5)] to the phase variables [the θ_j of Eq. (6)]. As it happens, for overdamped arrays [$\beta_c=0$ in Eq. (5)] the explicit transformation is known [16]. Similarly, in the classic problem of weakly coupled, weakly nonlinear oscillators, the required transformation is that from Cartesian to polar coordinates, and the phase variables θ_j is simply the polar angle [17].

Going back to Eq. (6), if the load is not strongly resonant, then the circuit equations can be analyzed using a weak-coupling averaging method. The resulting dynamics maps onto the Kuramoto model [16], where the coupling strength K embodies the load response but is independent of how many junctions are synchronized. Said differently, in this weak-coupling limit, the coupling constants K and α depend only on the bare frequencies of the individual junctions, irrespective of the frequency-pulling induced by the load. This stands in contrast to the behavior of the full, unaveraged dynamics when the load has a high Q , since then the locked and unlocked junctions affect the coupling differently. We can take account of this effect by making the coupling strength dependent on i as follows:

$$\dot{\theta}_j = \omega_j - (1/N_a) \sum_{i=1}^{N_a} \frac{N_a}{N} K_i \sin(\theta_j - \theta_i + \alpha), \quad (7)$$

where K_i takes on a large value \bar{K} if the i th oscillator is locked, and otherwise has a relatively smaller value K . (We have split off the ratio N_a/N for later convenience.) Notice that the sum is only over all active junctions, since only these drive the load in the first place. In essence, this modification of the Kuramoto model is a simple way to take into account the dynamical nature of the coupling “constant” without expanding the phase space to include additional dynamical variables.

Let us now consider the consequences of the new wrinkle to the collective synchronization. We can readily see that this modified Kuramoto model reproduces the basic feature of Fig. 1. As oscillators are activated one by one, the coupling term builds slowly. At some point, the load is active enough to lock one oscillator, at which point the corresponding coupling constant jumps, increasing the magnitude of the nonlinear interaction, and making it more likely to lock one or more additional oscillators. If the jump is large enough, this can cause a cascade, with several oscillators suddenly locking at the critical value of N_a (see below).

To make these ideas quantitative, we suppose that the ratio between the two values of the coupling constant is determined by the ratio between the response of the resonance at the two frequencies, the bare frequency of the unlocked oscillators ω_0 and at the resonance Ω [see Eq. (5)]:

$$\frac{\tilde{K}}{K} = \sqrt{\frac{(\omega_0/\Omega)^2 - 1}{L\Omega/R}}. \quad (8)$$

Here the fact that we have modeled the system using the analytically tractable Kuramoto form becomes useful. As long as the order parameter r is zero the system remains in a state corresponding to the lower coupling constant K . This state is stable up to a critical value of the coupling constant K_c equal to the width of the natural frequency distribution 2γ [6] (recall γ is the half width of the natural frequency distribution), so we can promptly derive the onset of instability of the $r=0$ and thus estimate \tilde{N}_a , the threshold number of oscillators above which some frequency locking will first occur. This estimate is made simply by writing the condition for the critical coupling constant corresponding to the lower K value, and solving for the number of active oscillators:

$$\frac{N_a}{\tilde{N}_a} K > 2\gamma \Rightarrow \tilde{N}_a \approx \frac{N}{K} 2\gamma. \quad (9)$$

When the state $r=0$ becomes unstable in the standard model (6) the order parameter smoothly increases as $r \approx \sqrt{1 - 2\gamma/K}$. Instead, in the new model (7) the higher value of the coupling must be used, and therefore the value of the order parameter r just after the threshold is

$$r \approx \sqrt{1 - \frac{2\gamma}{\tilde{N}_a \tilde{K}/N}} = \sqrt{1 - \sqrt{\frac{L\Omega/R}{(\omega_0/\Omega)^2 - 1}}}. \quad (10)$$

In other words if the ratio 8 is large enough, we expect a sudden jump from $r=0$ to $r \approx 1$ at the critical value \tilde{N}_a . This is just what we see in our simulation of the Josephson array (Fig. 1).

If we now imagine decreasing again the number of active oscillators, eventually the $r=0$ state becomes stable again because there are too few active oscillators N'_a . Setting $r=0$ yields

$$\frac{N'_a}{N} \tilde{K} < 2\gamma, \quad (11)$$

and so, from Eq. (8),

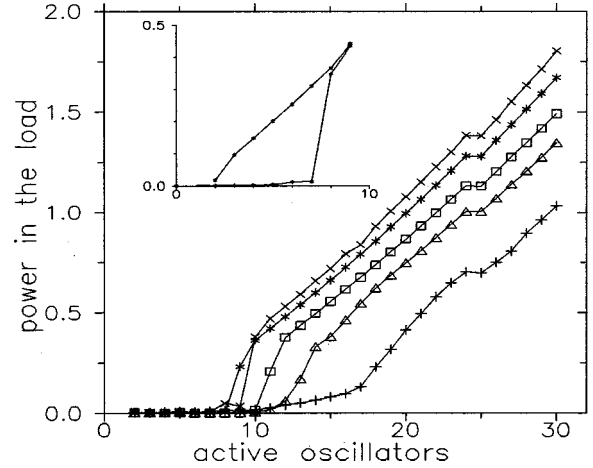


FIG. 5. Power in load (in normalized units) vs the number of active junctions for various cavity Q 's for a parallel array. Parameters of the simulations are $N=30$, $\beta=10$, $\gamma=0.003$, $\delta=0.006$, $\beta_L=1$, $Q=25$ (crosses), 50 (pluses), 75 (triangles), 100 (squares), and 200 (stars). The inset shows the lower part of the case $Q=400$.

$$N'_a < \tilde{N}_a \sqrt{\frac{L\Omega/R}{(\omega_0/\Omega)^2 - 1}}. \quad (12)$$

It follows that this restabilization of the $r=0$ case will occur at a number of active oscillators lower than the first threshold [Eq. (9)]. Exactly how much lower depends on the relative amplitudes of the resonance at the two frequencies (8). In conclusion, we predict that there will be a coexistence of two stable solution branches, one corresponding to very weakly coupled (and unsynchronized) oscillators and the other corresponding to a finite value of the order parameter when the number of active oscillators is in between Eqs. (12) and (9).

IV. CONSEQUENCES OF THE GENERAL MODEL

The preceding discussion shows that the synchronization behavior observed in the Josephson arrays is captured by the modified Kuramoto model (7). The key element is that the coupling “constant” is significantly enhanced for a locked oscillator; physically, the source of this enhancement is the highly resonant cavity. Our general picture implies that the observed “turn on” of locking will be more pronounced the sharper the resonance of the cavity, since this increases the difference between \tilde{K} and K . This is precisely what we observe in our simulations of the full circuit equations, as shown in Fig. 5. As the cavity Q is raised, the rise of synchronization above the transition point gets steeper. We see that for some (lower) values of Q , the load power turns on in a way that appears approximately quadratic Eq. [7], but for larger values the onset is nearly vertical. Notice, too, that the threshold N_{th} shifts down with increasing Q , since the necessary condition for the onset of synchronization is that the load is driven hard enough to overcome the cavity power losses (and increasing Q decreases these losses). From these observations, we conclude that the dependence of the ac power, P_{ac} , on the number of phase-locked junctions is non-trivial. For the parameter values used in Fig. 5 we can plot N_{th} vs $1/Q$ and extrapolate to $1/Q \rightarrow 0$, and find the limiting

value of $N_{th} \approx 5$ corresponding to the dissipation in the junctions.

Yet another interesting effect can be seen in Fig. 5 at $N_a = 24$. It turns out that, for this realization of randomness used in Fig. 5, the 25th junction has an exceptionally low critical current (some 1/4 of the mean). What happens, and is clearly reflected in the figure, is that this junction never frequency locks. Thus, the rise in the load power simply “misses a beat” but otherwise continues its steady rise as further junctions are activated (and synchronized). This type of “defect” could be easily observable in laboratory experiments, since quite typically a large Josephson array will contain a few percent of very poor junctions.

We emphasize that the outcome of the randomization of the supercurrent has but little influence on the threshold curves as those shown in Fig. 5. For one of these curves we tried with ten different randomizations (same width) and the threshold curves deviated at most by one junction.

The inset of Fig. 5 demonstrates that something happens at very large cavity Q , namely the appearance of a pronounced hysteresis, just as expected from our analysis of the general model. The figure shows what happens as junctions are successively activated up to $N_a = 30$, and then successively in reverse order. (A junction was deactivated by resetting its initial conditions and raising its critical current to a very high value $I = 10$.) We see that the synchronized state persists, thanks to the large oscillations of the load, which are able to provide adequate driving to synchronize the remaining active junctions. Such hysteresis was observed in recent studies [18] of a Kuramoto-type model using underdamped oscillators [i.e., adding a mass term $m\ddot{\theta}_j$ to Eq. (6)] and was also reported in coupled mechanical oscillator systems [4].

Finally, Fig. 6 summarizes our results for how N_{th} depends on what are the key physical elements of this cavity-induced synchronization mechanism. Recalling Fig. 3, the important parameters are the width of the cavity resonance $1/Q$, the detuning between the mean oscillator natural frequency δ , and the width of this natural frequency distribution γ . The threshold for synchronization is lowered by either decreasing the cavity losses (decreasing $1/Q$) or decreasing the cavity-oscillator mismatch (decreasing δ). (Negative δ negative leads to phase lock in the out-of-phase mode and therefore the present feedback mechanism does not work.)

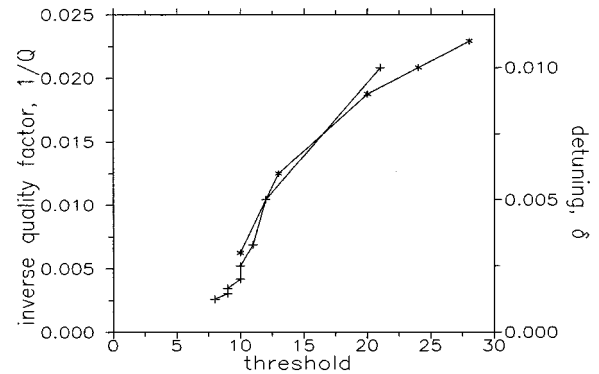


FIG. 6. Threshold value of N_a vs the inverse cavity factor $1/Q$ (pluses, left axis) for $\delta = 0.006$ and vs the normalized frequency detuning δ (squares, right axis) of a parallel array for $Q = 100$. Parameters of the simulations are $N = 30$, $\beta = 10$, $\gamma = 0.003$, $\beta_L = 1$.

Both of these amount to systematically increasing the interactions; in contrast, merely by increasing the width γ has little systematic effect on N_{th} , though it may increase the scatter over different realizations. Here we do not show the effect of γ because for this set of parameters it has simply no effect on the threshold.

In conclusion, the model presented in this paper describes the recent experiments [7] on power radiation from Josephson junction arrays in a cavity very well. The features of the synchronization behavior can be understood in generic dynamical terms as embodied by a modified Kuramoto model. We also predict that some hysteretic behavior should be observed if it is possible to turn off active (and synchronized) oscillators, a feature that is not possible in the Josephson junctions experiments of Ref. [7]. The strongly resonant cavity provides the key mechanism for junction-junction interactions, a property familiar in other coherent physical systems, e.g., gas lasers [7,10–12].

ACKNOWLEDGMENTS

We gratefully acknowledge P. Barbara and C. Lobb for extensive discussions and for sharing their experimental results prior to publication. We also thank T. Bohr, S. Benz, T.A.B. Kennedy, and J. Mygind for useful discussions. K.W. and G.F. thank the DTU Department of Physics for its hospitality.

[1] A.T. Winfree, *The Geometry of Biological Time* (Springer, New York, 1980).
 [2] S.H. Strogatz and I. Stewart, *Sci. Am. (Int. Ed.)* **269**, 102 (1993).
 [3] S.H. Strogatz, *Norber Wiener's Brain Waves*, in *Lecture Notes in Biomathematics Vol. 100* (Springer, New York, 1994).
 [4] I.I. Blekhman, *Synchronization in Science and Technology* (ASME Press, New York, 1988).
 [5] *Active and Quasi-Optical Arrays for Solid State Power Combining*, edited by R.A. York and Z. Popovich (Wiley, New York, 1997).
 [6] Y. Kuramoto, in *Proceedings of the International Symposium on Mathematical Problems in Theoretical Physics*, edited by

H. Araki, *Lecture Notes in Physics Vol 39* (Springer, Berlin, 1975); *Chemical Oscillations, Waves, and Turbulence* (Springer, Berlin, 1984).
 [7] P. Barbara, A.B. Cawthorne, S.V. Shitov, and C.J. Lobb, *Phys. Rev. Lett.* **82**, 1963 (1999).
 [8] R. Monaco, N. Grønbeck-Jensen, and R.D. Parmentier, *Phys. Lett. A* **151**, 195 (1990).
 [9] A. Davidson, N. Grønbeck-Jensen, and N.F. Pedersen, *IEEE Trans. Magn.* **27**, 3347 (1991).
 [10] R. Bonifacio, F. Casagrande, and M. Milani, *Lett. Nuovo Cimento Soc. Ital. Fis.* **34**, 520 (1982).
 [11] S.G. Lachenmann, T. Doderer, and R.P. Huebener, *Phys. Rev. B* **56**, 5564 (1997).

- [12] D.R. Tilley, Phys. Lett. **33A**, 205 (1970).
- [13] G. Filatrella, G. Rotoli, N. Grønbeck-Jensen, R.D. Parmentier, and N.F. Pedersen, J. Appl. Phys. **72**, 3179 (1992).
- [14] S. Nichols and K. Wiesenfeld, Phys. Rev. A **45**, 8430 (1992).
- [15] H. Sakaguchi and Y. Kuramoto, Prog. Theor. Phys. **76**, 576 (1986).
- [16] K. Wiesenfeld, P. Colet, and S.H. Strogatz, Phys. Rev. Lett. **76**, 404 (1996); Phys. Rev. E **57**, 1563 (1998).
- [17] N. Minorsky, *Nonlinear Oscillations* (van Nostrand, Princeton, 1962).
- [18] H.A. Tanaka, A.J. Lichtenberg, and S. Oichi, Phys. Rev. Lett. **78**, 2104 (1997); Physica D **100**, 279 (1997).